Poyang Hu (Jiangxi Province, P. R. of China) Area Variations between January 2004 and June 2006 Using ENVISAT Low and Medium Resolution Time Series

Andreoli R. [1], Yésou Y. [1], J Li [2], Desnos Y-L. [3], Shifeng H. [2], De Fraipont P. [1]

[1] SERTIT, Université Louis Pasteur, Bld Sébastien Brant, BP 10413 F-67412 Illkirch-Graffenstaden, France,
E-mail: remi@sertit.u-strasbg.fr
[2] IWHR, Ministry Water Resource, Beijing, China
E-mail: lijiren@iwhr.com; huangsf@iwhr.com
[3] European Space Agency-ESRIN, Italy
E-mail: Yves-louis.desnos@esa.int

Abstract

Poyang Hu, one of the most regularly flooded areas in China, can be considered as a key hydrological element in flood control and reduction within the middle Changjiang basin. This area was selected as a major test site of the Flood DRAGON Project, part of the MOST-ESA DRAGON Programme. Over two and half years, water extent was monitored based on sixty-four ENVISAT low and medium resolution ASAR and MERIS FR images. It's the first time that such an amount of ENVISAT data was used in monitoring inland lake water extent variations. This original integration approach involves: lake surface variation analysis, yearly submersion time estimation, and a spatial recognition of three major hydrological sub-systems. The results highlight the great potential of ENVISAT, and more largely Earth Observation Medium Resolution data, for large inland water body monitoring and management. This approach can be applied worldwide in the context of global climate change.

Keywords

Poyang Hu, floods, submersion time, ENVISAT, ASAR, WSM, MERIS FR, earth observation time series, hydrological dynamics.

I. INTRODUCTION

Floods are one of the most important natural disasters regularly causing large amounts of casualties together with increasing economic losses. Worldwide, China is one of the countries in which flooding occurs the most frequently. The Poyang Hu area, considered as an hydrological key component in flood control and reduction in the middle Changjiang basin is one of the most regularly flooded areas in China.

Poyang Hu was selected as the principal test site of the Flood DRAGON Project, part of the MOST-ESA DRAGON Programme focussed on science and applications development in China using mainly data from the ERS and ENVISAT missions(Desnos, et al., 2004; Desnos, et al., 2006). The aim of the Flood DRAGON Project is to explore the potential of ENVISAT ASAR and MERIS data, in terms of spatial and temporal resolution, applied to rapid flood mapping and monitoring(Yésou, et al., 2004; Li, et al., 2006). A second level purpose of the Flood DRAGON project consists of extending and improving floods management methods and tools plus hydrological balance analysis in terms of prevention and forecasting using space technologies(King, et al., 2004).

Over the Poyang Hu, a considerable database was set up including a large number of ENVISAT Products, Advanced-SAR(ASAR) ranging from global to high resolution, and MERIS Full Resolution optical data, acquired between January 2004 and June 2006. This database is completed by high resolution Landsat, SPOT data, CHRIS PROBA(Yésou, et al., 2004) and topographical SRTM data. One of the first innovative aspects of the Flood DRAGON project was to explore the potential of low resolution ASAR Global Monitoring Mode (GMM) products for regional landscape characterization and regional water body monitoring(Andreoli, et al., 2006.) Mostly exploited for ice mapping and monitoring(Pedersen, et al., 2005), a set of sixteen GMM acquired between February 2004 and April 2005 showed the potential of this data type for large inland water surface analysis. This study also led to three major land cover types being distinguished: permanent water bodies during the period, areas of seasonal water level variations, and wet lowlands mostly consisting of paddy fields and marshes. Furthermore, a preliminary annual dynamic analysis of the Poyang Hu has been generated(Andreoli, et al., 2006).

This paper presents an analysis of Poyang Hu surface variations based on an innovative approach exploiting ENVISAT data time series with the integration of ENVISAT optical and ASAR medium resolution products (MERIS and ASAR Wide Swath Mode). The study is focussed firstly on the assessment of the synergy between multi-source and multi-resolution earth observation data time series for flood mapping and monitoring. Sixty-four earth observation images during a three year period over the Poyang Hu region were analysed and compared amongst themselves and with high resolution earth observation data. An estimation of the yearly submersion time of the Poyang Hu based on ENVISAT data time series analysis is proposed, allowing a preliminary spatial characterization of water dynamic inside the lake.

1082-4006/07/13(01-02)-24$5.00

II. STUDY CONTEXT

A. Poyang Hu study site

Located in Jiangxi Province, Poyang Hu is the largest freshwater lake in China and constitutes a major hydrological subsystem of the middle Changjiang basin in Central China. It extends in a hollow depression in the north of the Province at very low elevation, only about ten meters above sea level, surrounded by several mountain chains.

The climate of the Poyang Hu region is subtropical humid with monsoon. Annual mean rainfall is between 1200 and 2400 millimetres and precipitations are concentrated between April and July[9].

The area which Poyang Hu covers is about 162,000 km² and includes Jiangxi Province's major rivers, Xiushui, Gan, Fuhe, Raohe and Xin, flowing from the south of Jiangxi province to the north into Poyang Hu. Poyang Hu has only a narrow outlet into the Changjiang which lies on the northern border of the province(Figure 1). Poyang Hu undergoes very significant seasonal water level variations: the water level varies between 9 and 18 m and its size fluctuates from less than 1,000 km² during the dry winter period to more than 4,000 km² during the wet summer period.

During a normal hydrological year, the discharge peak of the Jiangxi river occurs between April and June during the rainy season, raising the lake's water level. The discharge decreases from July to September but, at the same time, the water level of the Changjiang increases. As a result, the drainage from the lake to the Changjiang River reverses and begins moving from the Changjiang into Poyang Hu about mid-July(Shankman, et al., 2003). Thus, Poyang Hu and the lower section of the tributary rivers flood most years during the summer months. The major floods occur when high discharge from the Jiangxi rivers and Changjiang coincide. Seven major floods have occurred in the past fifty years (1954, 1973, 1977, 1983, 1992, 1995, 1998) and the most severe ever recorded was in 1998 (Shankman, et al., 2006).

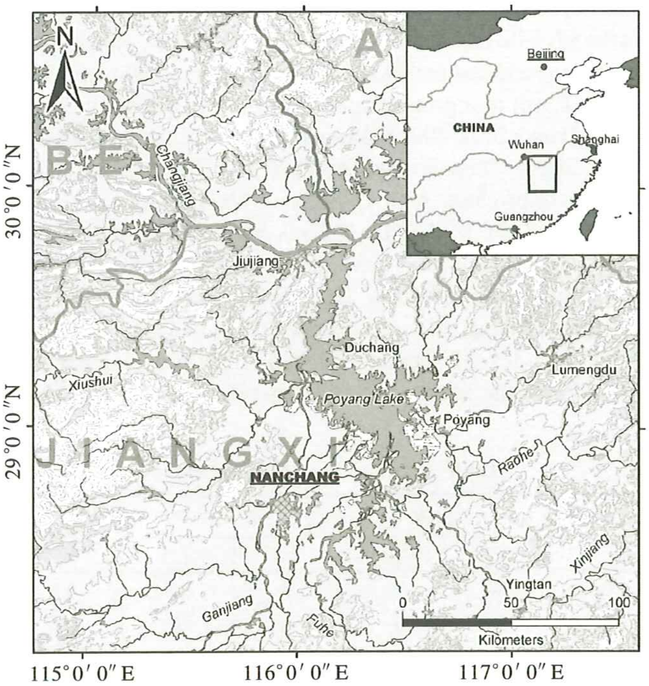

Figure 1. Location map

Poyang Hu is surrounded by large wetlands of floodplain and marshlands (lakeshore) of which a large part has been reclaimed as farmland in the past hundred years(Jiang, et al., 2005). After the dramatic floods of 1998, Chinese government established a wetlands restoration policy.

B. The use of earth observation time series for flood monitoring

The capabilities of remote sensing in flood mapping and monitoring are well recognized. The first studies and applications were developed using optical data after the launch of the first sensors(Smith, 1997). Optical data quality depends on cloud cover but radar remote sensing has an "all weather" monitoring capability, and its wide coverage is an important tool for flood monitoring(Tholey, et al., 1997., Laugier, et al., 1997; Chen, et al., 1999; Mahmood, et al.,1999; Sarti, et al., 2001; Yésou, et al., 2001). These capabilities were well demonstrated during the 1998 and 1999 flood events in China when Radar remote sensing played a very important role in flood disaster monitoring and evaluation(Xu, et al., 2003; Zhou, et al., 2000; Li, et al., 2003).

Major floods, such as the 1988 Ganges-Brahmaputra and the 1998 Changjiang floods, were monitored based on the exploitation of coarse data (spatial resolution about one kilometre) such as NOAA AVHRR(Islam, et al., 2000; Liu, et al., 1999; Liu, et al., 2002; Zhou, et al., 2000; Gao, et al., 2001).

Only a few examples of flood monitoring based on high or medium resolution time series data from earth observation satellites are presented in the literature. Most cases concern discontinuous monitoring of a flood plain exploiting a small number of images (*ie* less than 10) acquired in critical hydrological periods (low and high water level(Tan, et al., 2004)). Otherwise, studies exploiting a longer data time series (*ie* more than 20 images) cover only a single disaster event (Laugier, et al., 1997; Yésou, et al., 2000).

However, two interesting studies were recently conducted over similarly complex hydrological systems based on medium resolution data time series. The first concerns MERIS data processing for land cover changes and flood characterization in the Niger delta region(Seiler, et al., 2003). The second consists of area variation studies and sedimentation pattern monitoring over the Poyang Hu using a set of 30 MODIS medium resolution data covering the 2003 and 2004 hydrological years(Qian, 2006).

III. DATABASE AND METHODS

A. Data base over Poyang Hu area

The database over Poyang Hu area includes firstly a set of optical high resolution reference data (2 Landsat, 6 SPOT 4, and 1 CHRIS-PROBA coverage) acquired at different hydrological periods and a 3 arc-second (90m) SRTM Digital Elevation Model.

Table 1. Reference EO optical data

satellite	Type	date	Hydrological period
Landsat 5 TM	Multispectral	15/07/1989	High water level
Landsat 7 ETM+	Multispectral	10/12/1999	Low water level
SPOT 4	Multispectral	08/08/1998	Floods
SPOT 4	Multispectral	23/11/2004	Draw-off
SPOT 4	Multispectral	02/04/2005	Infilling
SPOT 4	Multispectral	15/07/2005	High water level
SPOT 4	Multispectral	16/10/2005	Draw-off
SPOT 4	Multispectral	07/01/2006	Low water level
CHRIS PROBA	Multispectral	22/06/2005	High water level

Landsat reference data have been used for a preliminary hydrodynamic characterization of Poyang Hu's annual water level variations and land cover mapping(Figure 2). Water bodies and wetland areas have been extracted by thresholding each Landsat image. Lowlands, including lands below 20m mean sea level height and frequently flooded overbanks, have been discriminated using SRTM DEM and medium scale landscape analysis. The resulting classification shows the annual water level dynamics while differentiating low water levels, areas of seasonal water variations (lakeshore) and wetland soils associated with lowlands(Figure 2).

SPOT 4 high resolution optical data have been acquired within the framework of the Sino-French WARM cooperation programme(King, et al., 2004) and they cover the Kangshan area(centre-east part of the Poyang Hu). Five multispectral SPOT 4 data were acquired for each major stage of the Poyang Hu dynamic between November 2004 and January 2006 (infilling, high water level, draw-off, low water stage), and the last one was recorded during the dramatic 1998 floods.

The ENVISAT database includes a total of sixty-four images acquired between January 2004 and June 2006 with an average temporal revisit of about 11 days: 14 ASAR Global Monitoring Mode (GMM), 16 ASAR Wide Swath Mode (WSM) and 34 MERIS products (13 Level 1 and 21 Level 2).

The Global Monitoring Mode, like the Wide Swath Mode, is based on the ScanSAR technique using five sub-swaths of ENVISAT either in HH or in VV polarization. These two modes offer datasets with swath coverage of up to 405 km. The spatial resolution of GMM data is 1 km for a pixel spacing of 500 m by 500 m while WSM spatial resolution is 150 m for a pixel spacing of 75 m by 75 m(ESA, 2002).

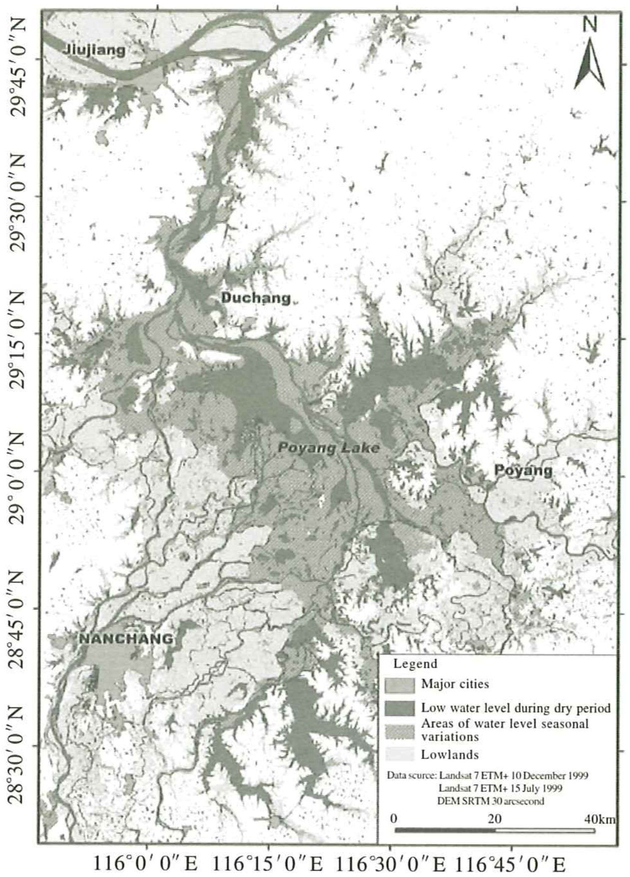

Figure 2. Landsat land cover of the Poyang Hu area

The Medium Resolution Imaging Spectrometer (MERIS) loaded on the ENVISAT satellite is a 68.8° field-of-view, push-broom, imaging spectrometer that measures the solar radiation reflected by the Earth at a ground spatial resolution of 300 m, in 15 spectral bands in the 390–1040 nm range(visible and near infrared) (ESA, 2004). There are two levels of MERIS product. Level 1 consists of products with 15 radiance channels of visible and near infrared. The MERIS Level 2 processor uses specific modules according to cloud, land or water surfaces in order to generate geophysical image products. The first 15 bands of MERIS Level 2 products correspond to raw channels converted into reflectance. In addition, level 2 products contain 16 geophysical products derived from the 14 reflectance channels(ESA, 2004).

Table 2. ENVISAT data time series

	ASAR		MERIS FR		Total
	GMM	WSM	L1	L2	
2004	14	5	5	13	37
2005	0	4	6	8	18
2006	0	7	2	0	9
Total	14	16	13	21	64

B. Data processing

Analysis of the ENVISAT data time series is based on a processing chain with three major steps(Figure 3) including a pre-processing step of data calibration and geometric corrections, the extraction and validation of water bodies, and finally, the estimation of submersion time using the average of a water presence/absence monthly mean.

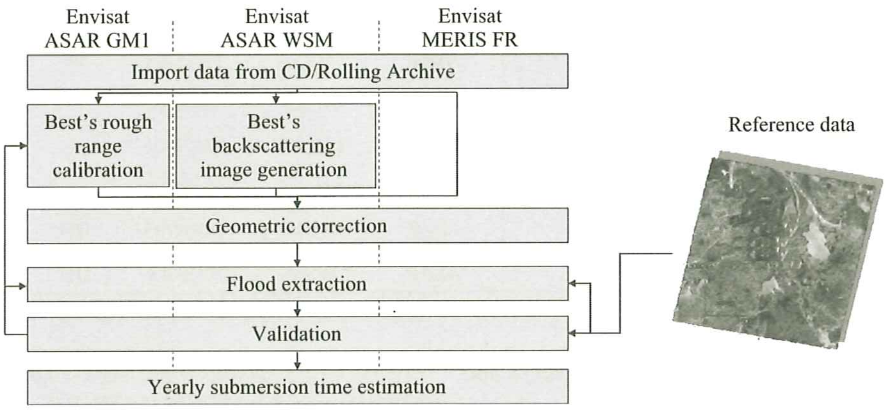

Figure 3. Processing chain

(i) ENVISAT data calibration and geometric correction

Low and medium resolution ASAR products must be corrected for antenna pattern effects. Global Monitoring Mode and Wide Swath Mode data were corrected for antenna pattern effects using, respectively, the *Rough-range calibration tool* and the *backscattering image generation tool* of the Basic ENVISAT SAR Toolbox (BEST) software(ESA, 2005). *Rough-range calibration* processing does not correspond to a "true" calibration, so GMM data were then standardized to make them comparable.

Geometric correction techniques have been adapted according to product type. Due to the coverage and resolution of Global Monitoring Mode products, these are georeferenced using a second order polynomial model using ERDAS Imagine v8.7. On the other hand, Wide Swath Mode data have been orthorectified using an SRTM digital elevation model in PCI Geomatica v9.1. With respect to MERIS data, the orthorectification tool of VISAT (BEAM 3.4.1 software) was used with GETASS digital elevation model[34]. This latter tool provides good results when considering data resolution and terrain configuration (relatively flat areas).

(ii) Water body extraction and validation procedures

In ENVISAT ASAR data, the low backscattering characteristic of water, which usually appears with a dark tone on SAR imagery, was used to extract water by pixel-based thresholding. In the case of windy conditions or partially submerged vegetation, the backscattered signal can be affected presenting higher backscattering values(Tholey, et al., 1997; Yésou, et al., 2001). In these cases, the water layer was manually corrected by the operator.

Due to the difference between MERIS Level 1 and Level 2 product characteristics, water extraction techniques are not similar. A preliminary pixel assignment of the surface type (cloud, land or water) is made during MERIS Level 2 product generation(ESA, 2004). As a result, water extraction on MERIS FR Level 2 products is made easier and a single threshold using either band 10 or band 13 (Near Infrared) was performed. Two methods were jointly used in order to extract water bodies according to the hydrological period when using MERIS Level 1 products. During the low water level period, a single threshold using band 14 (Near Infrared) was performed. During the high water level period, the lakeshore covered by grassland is flooded leading to differences in radiometry within water. The $NDVI_{mean}$, using formula (1), is less sensitive over these different types of water than a single channel. It was therefore used to extract water bodies by thresholding.

$$NDVI_{mean} = \frac{\frac{1}{n_{pir}}\sum_{i=10}^{15} DN - \frac{1}{n_{red}}\sum_{i=6}^{9} DN}{\frac{1}{n_{pir}}\sum_{i=10}^{15} DN + \frac{1}{n_{red}}\sum_{i=6}^{9} DN} \quad (1)$$

$$With: \begin{cases} i = \text{band number} \\ DN = \text{reflectance value} \\ n_{pir} = \text{number of near infrared bands} \\ n_{red} = \text{number of red bands} \end{cases}$$

The validation of water extent extracted from ENVISAT products was performed in two stages. Optical high resolution data, such as SPOT 4 data, is known in literature to allow an accurate discrimination of flood boundaries(Smith, 1997). The water extracted from ENVISAT data were firstly compared with water extracted from SPOT 4 data by a supervised classification. The overlay between ENVISAT water and SPOT 4 water was calculated in percent at the coarser resolution for each pair of water extents. The comparison was made between different data acquired approximately at the same period (gap comprised between 0 and 15 days) to minimize errors due to the dynamic

Table 3. List of SPOT and ENVISAT water extent pairs that were compared

Water extend extracted from:					... is compared to water extend extracted from:					ΔD[3]
Sensor	product	date	P[1]	mode	Sensor	product	date	P[1]	mode[2]	
SPOT	XI	23/11/04	–	–	ASAR	GMM	23/11/04	HH	A	0
SPOT	XI	23/11/04	–	–	MERIS	FR_L2	24/11/04	–	D	1
SPOT	XI	23/11/04	–	–	ASAR	WSM	15/11/04	VV	D	8
SPOT	XI	03/04/05	–	–	MERIS	FR_L1	03/04/05	–	D	1
SPOT	XI	17/07/05	–	–	MERIS	FR_L2	17/07/05	–	D	2
SPOT	XI	17/10/05	–	–	MERIS	FR_L2	17/10/05	–	D	1
SPOT	XI	14/01/06	–	–	ASAR	WSM	14/01/05	HH	A	7
SPOT	XI	20/01/06	–	–	ASAR	WSM	20/01/06	HH	A	13

Note: 1. Polarization; 2. Ascending (A) or Descending (D); 3. Number of days between compared images

of Poyang Hu. A total eight pairs were compared (1 SPOT and GMM, 3 SPOT and WSM, and 4 SPOT and WSM).

Equally, the synergy between water bodies extracted from ENVISAT ASAR and MERIS data was estimated by calculating in percent the overlay between the different extracted water layers. Comparisons were separated by data type couples: MERIS and ASAR GMM; MERIS and ASAR WSM and; ASAR WSM and ASAR GMM. Fifteen data pairs were compared (7 MERIS and ASAR GMM; 4 MERIS and ASAR WSM and; 4 ASAR WSM and ASAR GMM) for which acquisition dates were separated by eleven days at the most (Table 4).

Table 4. List of compared ENVISAT GMM, WSM and MERIS water extent couples

Water extend extracted from:					... is compared to water extend extracted from:					ΔD[3]
Sensor	product	date	P[1]	mode	Sensor	product	date	P[1]	mode[2]	
ASAR	GMM	25/07/04	HH	A	MERIS	FR_L2	17/07/04	–	D	8
ASAR	GMM	25/07/04	HH	A	MERIS	FR_L2	23/07/04	–	D	2
ASAR	GMM	26/08/04	HH	A	MERIS	FR_L2	27/08/04	–	D	1
ASAR	GMM	06/09/04	HH	D	MERIS	FR_L2	12/09/04	–	D	6
ASAR	GMM	19/10/04	HH	A	MERIS	FR_L2	17/10/04	–	D	2
ASAR	GMM	23/11/04	HH	A	MERIS	FR_L2	24/11/04	–	D	1
ASAR	GMM	09/12/04	HH	A	MERIS	FR_L1	10/12/04	–	D	1
ASAR	WSM	21/02/06	HH	A	MERIS	FR_L1	03/03/06	–	D	10
ASAR	WSM	27/04/06	HH	D	MERIS	FR_L1	1704/06	–	D	10
ASAR	WSM	21/08/04	HH	D	MERIS	FR_L2	27/08/04	–	D	6
ASAR	WSM	11/09/04	HH	A	MERIS	FR_L2	12/09/04	–	D	1
ASAR	GMM	27/04/04	VV	A	ASAR	WSM	30/04/04	HH	A	3
ASAR	GMM	26/08/04	HH	A	ASAR	WSM	21/08/04	HH	D	5
ASAR	GMM	06/09/04	HH	D	ASAR	WSM	11/09/04	HH	A	5
ASAR	GMM	31/12/04	HH	A	ASAR	WSM	20/12/04	VV	D	11

Note: 1. Polarization; 2. Ascending (A) or Descending (D); 3. Number of days between compared images

(iii) Submersion time estimation

Submersion time $P(w)$ is an average of the monthly mean of water surfaces expressed in percentage of year (2).

$$P(w)=\left(\frac{1}{12}\sum_{m=1}^{12}\left(\frac{1}{n_m}\sum_{t=1}^{n_m}w_{m,t}\right)\right)\times 100 \quad (2)$$

where
$$\begin{cases} P(w): \text{submersion time express in percent of year} \\ m: \text{month of the year} \\ n_m: \text{number of water extent layers of the month } m \\ w_{m,t}: \text{water extent layer extracted from ENVISAT} \\ \qquad \text{data for the month } m \text{ with } t\in[1;n_m] \\ \qquad \text{and } w_{m,t}\in\{0,1\} \end{cases}$$

Before calculating $P(w)$, the sixty-four ENVISAT water layers were down-sampled to 75 m resolution using a cubic spatial interpolation. The raw $P(w)$ map must be enhanced because of the differences in resolution of water surfaces extracted from ENVISAT. The coarser data(GMM and MERIS) lead to an under estimation of fine and small perennial water bodies but also to distortions of maximal water extent boundaries. Concerning these hydrological elements, a Landsat reference land cover map was used for the manual correction of the $P(w)$ map by visual interpretation.

IV. RESULTS AND DISCUSSION

This study is focussed on monitoring inland lake water extent variation. It is based on an innovative approach exploiting for the first time a large amount of ENVISAT data. Furthermore, the analysis allows for a spatial and regional overview of land submersion inside the Poyang depression. Principal results are concerned: assessment of ENVISAT MERIS and ASAR lake surface, lake variation over two and half years, estimation of annual submersion time, and a spatial recognition of Poyang Hu sub-systems.

A. ENVISAT ASAR and MERIS synergy in flood monitoring

Statistical analysis of ENVISAT water extent comparisons show that ENVISAT ASAR GMM, WSM and ENVISAT MERIS data are very efficient and that their water recognition concords(Figure 4 and Figure 5).

First of all, the comparisons of water bodies extracted from ENVISAT data and those obtained using SPOT 4 data(Figure 4) show that, on average, between 79.9 % and 88.6 % of the water detected by ENVISAT (ranging from the coarser to the most accurate data type) is also detected as water using SPOT 4 data. Hence, water extracted from ENVISAT data is very coherent with water detected by SPOT 4.

Commissions appear to be limited between 20 % for GMM

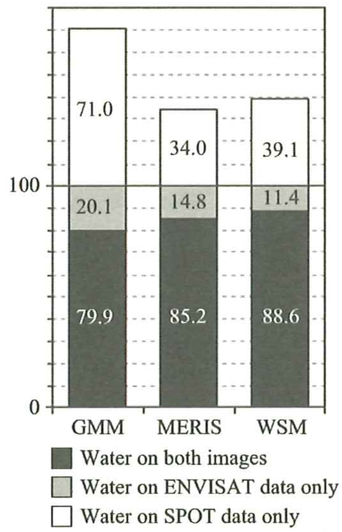

Figure 4. Comparison of water extents extracted from SPOT and ENVISAT data
(average of comparisons listed in table 3 expressed in percent)

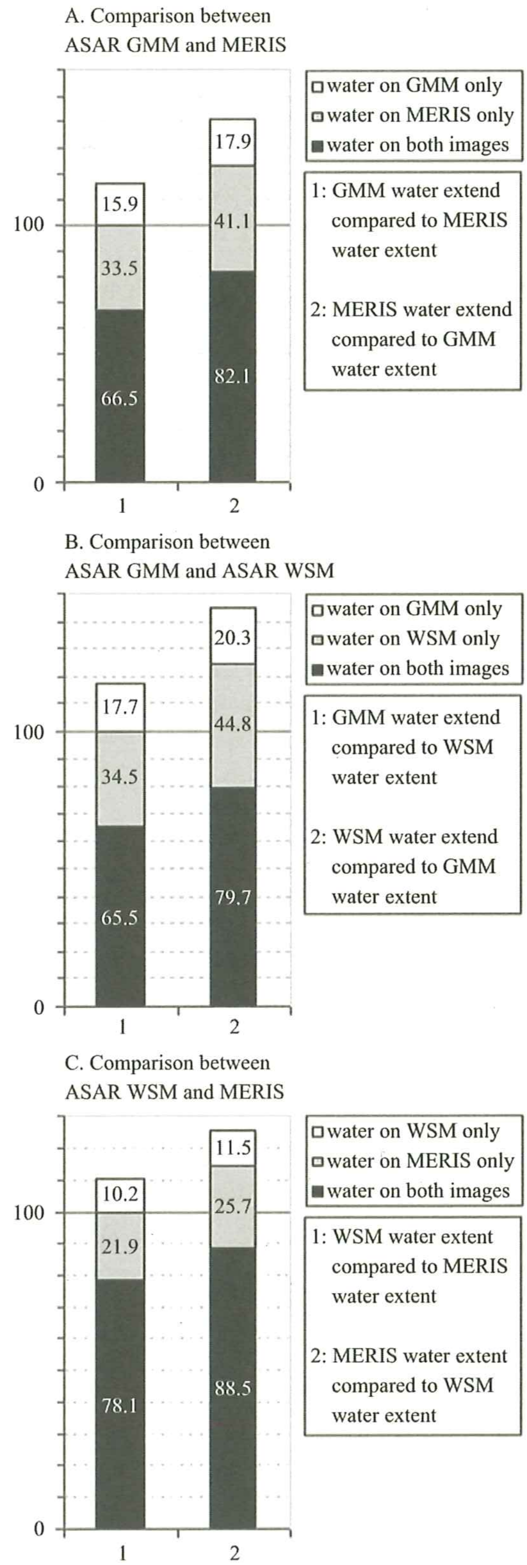

Figure 5. Comparison of water extents extracted from ASAR GMM, ASAR WSM and MERIS data
(average of comparisons listed in table 4 express in percent)

data to 11.4 % for WSM data. In general, SPOT 4 detects more water than ENVISAT: from 34 % more compared with MERIS, and 71 % compared with GMM.

The difference in resolution between ENVISAT data (ranging from 1km to 150m) and SPOT 4 data(20m) can explain these differences. In fact, the coarser data leads to under-estimating water extent at the edges of water bodies. On the contrary, the most accurate data is able to detect fine hydrological elements such as channels or small water bodies which explains that the percent of water detected only by SPOT decreases when ENVISAT resolution increases.

Comparing ENVISAT derived water bodies(Figure 5), the most interesting fact is that between 79.7 and 88.5 % of water extracted from the coarser resolution data is recognised on the better resolution data. Furthermore, the best concordance was obtained between ENVISAT WSM and ENVISAT MERIS data: 88.5% of WSM water extent is seen by MERIS and 78.1% of MERIS water extent is recognized by WSM data.

However, MERIS optical data tended to see more water in general than ASAR GMM and WSM data. This could result from the indistinct limits between water and very wet areas. Whereas visual comparison of water bodies' boundaries extracted from ENVISAT GMM, WSM and MERIS shows that external limits are distinct. Major differences are observed within large water bodies and correspond to alluvial terraces lining the delta's braided streams.

Thus, these differences are mainly due to resolution.

B. Poyang Hu surface variation between January 2004 and June 2006

The Poyang Hu extent was derived from sixty-four ENVISAT images acquired between January 2004 to June 2006(Table 5), and each water extent corresponds to lake state at the acquisition time. These were used to estimate Poyang Hu surface (in km²). Surface estimation was performed without taking account of Junshan Hu (south of Poyang Hu, estimated at 174.8 km²), which is considered without connecting with Poyang Hu. Also, rivers and small depressions around the lake were not taken into account.

Table 5. Poyang Hu water surface characteristics derived from ENVISAT data

	GMM	WSM	MERIS
Maximal lake surface (km²)	2939.00	2725.90	3103.83
Minimal lake surface (km²)	376.00	913.40	557.91
	Total		
Mean surface (km²)		1893.3	
Median surface (km²)		1863.7	

The smallest lake surface estimated for the period of monitoring was about 376 km². This surface was estimated from an ENVISAT GMM image acquired the 20th of February 2004 (polarization VV). The smallest surface recorded by MERIS data (557.91 km²) was during the same period (February 2004) and tends to illustrate a lower Poyang Hu level than normal. The biggest surface estimated is about 3103.8 km², from MERIS data acquired the 23rd of July 2004. During the 2004 and 2005 wet seasons, Poyang Hu surface exceeded 3000 km². The average Poyang Hu surface is estimated to be 1,893.3 km² for the monitoring period (between January 2004 and June 2006).

The size of Poyang Hu's surface derived from ENVISAT data various from the seasons appears related with Poyang Hu characteristics found in the literature(Shankman D, et al., 2003; Shankman D, et al., 2006)(Figure 6). The annual largest water extent occured during the flood season at the end of July for

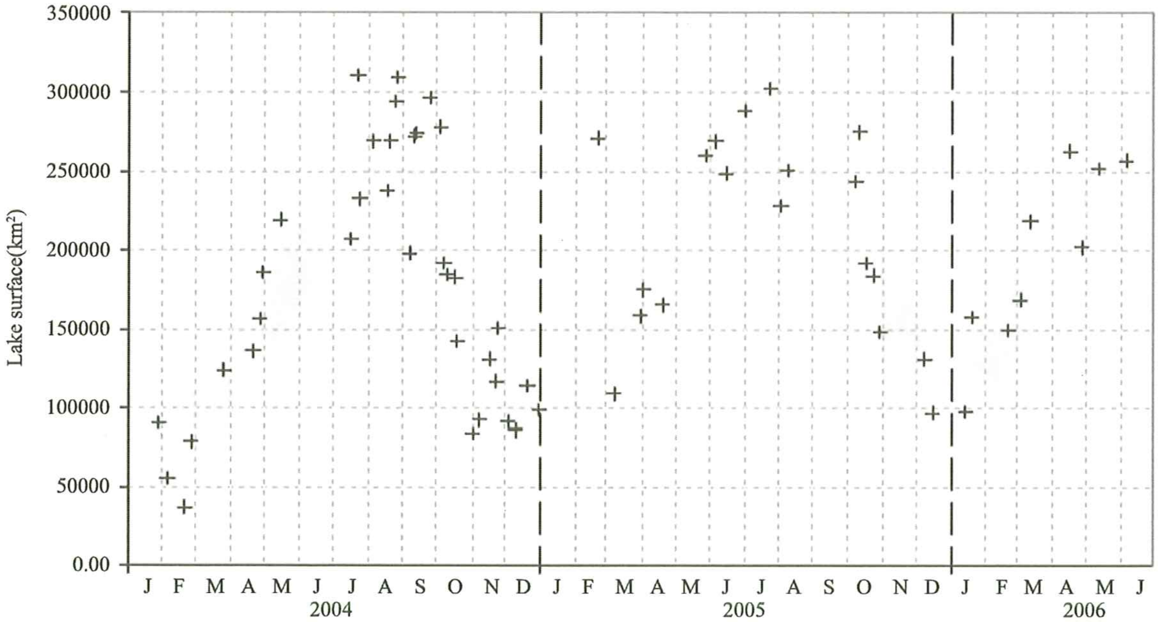

Figure 6. Poyang Hu variations observed by ENVISAT low and medium resolution data between January 2004 and June 2006

both 2004 and 2005. The lake surface is larger than 2500 km² generally from June-July to September(3–4 months). The lowest lake surface often occurs during the dry season at the end of December and during January. The lake surface is generally lower than 1,000 km² during the months of December and January.

The trends in Figure 6, show that the infilling of Poyang Hu starts at the end of February and beginning of March, and lasts over 4 months (March to June). On the contrary, the draw-off of the lake is abrupt (1–2 months). Starting at the end of September, Poyang Hu empties about 1000 km² in only 1 month (October) and reach 1500 km² at the beginning of November and less than 1000 km² in December. The area estimated for February 2005 is anomalous but corresponds to a flood peak(Andreoli, et al., 2006). The lake filled in 2006 as usual, but there was a drought in the summer of 2006 with a very low water level and consequently the size of Poyang Hu surface decreased.

Poyang Hu area variations calculated with ENVISAT low and medium resolution are in accordance with those obtained by Qian(Qian, 2006) for the year 2004 using MODIS medium resolution data(Figure 7). The two data sources show the same trends: the smallest lake surface was achieved in February 2004 and the largest lake surface was observed in July 2004. As observed with ENVISAT, the lake surface recorded by MODIS had reached its maximum between July and September with a slight decrease at the beginning of August. However, the Poyang Hu area estimated in March 2004 with MODIS is overestimated compared to ENVISAT.

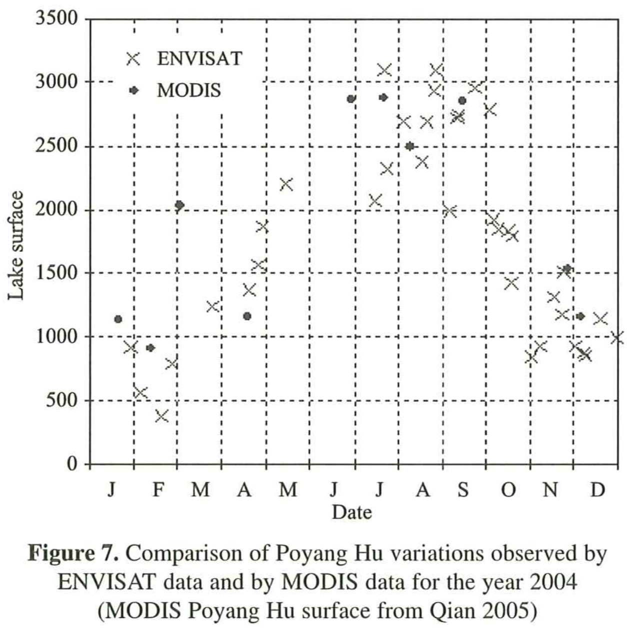

Figure 7. Comparison of Poyang Hu variations observed by ENVISAT data and by MODIS data for the year 2004 (MODIS Poyang Hu surface from Qian 2005)

The Poyang Hu monitoring begun in 2003 by Qian(Qian, 2006) have now been completed by this study for the year 2004, 2005 and the first half of 2006. These results highlight the great potential of ENVISAT and more generally Earth Observation Medium Resolution data for large inland water body monitoring and management.

C. Poyang Hu submersion time estimation between January 2004 and June 2006

The submersion time map corresponds in this study to a spatial and continuous representation of water presence between January 2004 and June 2006 expressed in percent of a year(Figure 8). It allows a quantitative description of lake variations but also a spatial characterization of yearly water fluctuations inside the Poyang depression.

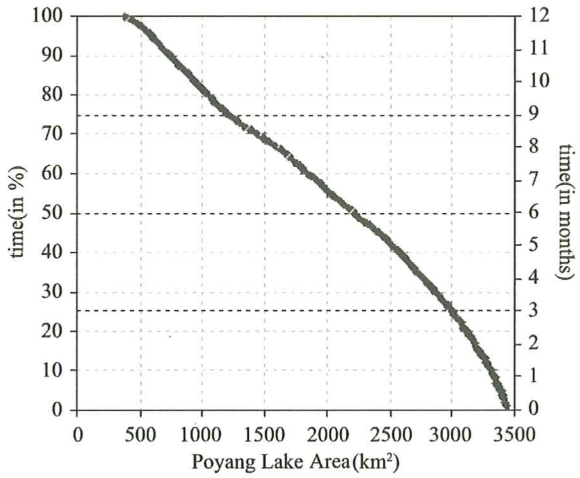

Figure 8. Cumulative frequency during yearly submersion time

The size of Poyang Hu, including perennial water bodies and areas of water level variations, was estimated at 3436.2 km² which is 332.4 km² greater than the maximal instantaneous major lake surface observed between January 2004 and June 2006. As previously mentioned analysing the ENVISAT GMM dataset, flooding events induce not only the simple dilation of water bodies but also a translation of flooded area inside the depression(Andreoli R, et al., 2006). During 3 months a year, the Poyang Hu area exceeds 3000.0 km²(Figure 8). And about 70 days a year the lake size is below 1000 km². Median lake area is about 2215.1 km² meaning that these areas are under water for half a year (183 days). Nearly 88% of the maximal size of the lake or 3057.3 km² corresponds to lakeshore (area of water level variations).

The estimated yearly submersion time is only representative of hydrological conditions of the analysed years since the year 2004 and 2005 were characterized by normal Poyang Hu water levels, and that the year 2006, as previously mentioned, was drier with very low water levels during the summer months.

D. Spatial recognition of Poyang Hu sub-systems

Poyang Hu is a major storage basin of the middle Changjiang reach. The water storage capability can be described, in terms of surface and time of water presence, using the estimate submersion time map. From a hydrological point of view, the

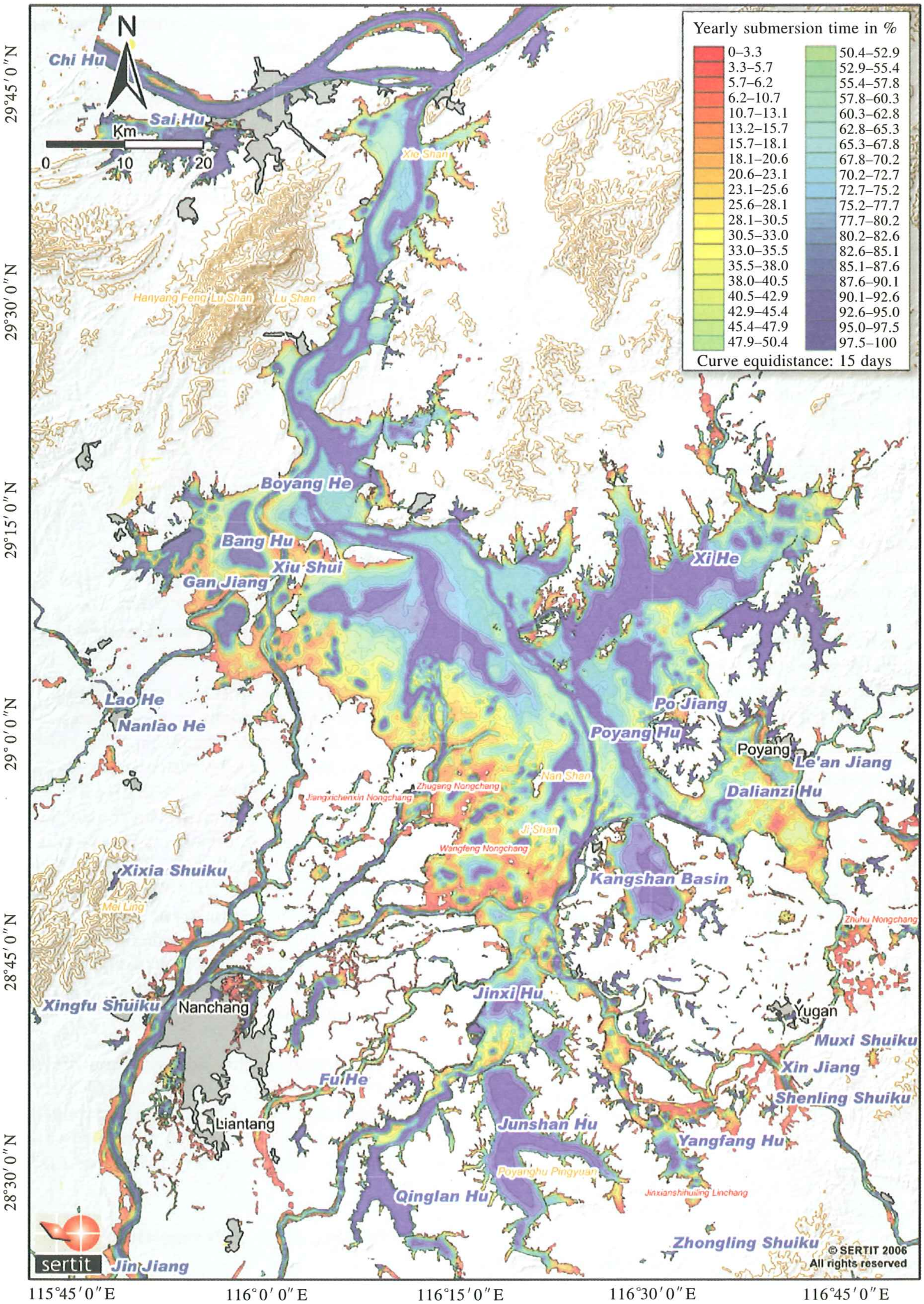

Figure 9. Poyang Hu submersion time estimation derived from ENVISAT low and medium resolution data time series acquired between January 2004 and June 2006

submersion time can distinguish the perennial hydrological elements (presence of water 100% of time) from the flood storage areas (presence of water less than 100% of time). According to the shape of perennial water bodies, water tanks and water transfer channels linking tanks inside the lake system can be identified. The spatial distribution of submersion time also highlights different storage areas according to the duration of water presence and their geographical location within the hydrological system.

In this way, Poyang Hu Basin can be divided into 3 major sub-systems(Figure 8): A. the channel linking the major basin of Poyang Hu to Changjiang river; B. small lateral lakes; C. the major basin of Poyang Hu which can be divided into 2 sectors according to a South-Eastern North-Western axis (C.1: Gan delta and Poyang Hu in the south-west and C.2: Xi He and Dalianzi Hu in the North-East).

The principal characteristics of these sub-systems are as followings:

A. The channel linking Poyang Hu to Changjiang river

Where perennial water bodies form braided streams. Most of the channel is under water nearly 50% of year. Only border fringes and lateral valley ends diverge from this.

B. Small lateral lakes

Such as Kangshan basin, Junshan Hu and Qinglan Hu lining Poyang Hu to the south-east, are perennial. Only small lateral valley ends present pronounced dynamics. In this sector, the Kangshan basin doesn't appear totally perennial, but this can be explained by the fact that vegetation usually grows on the edges of the basin and floats on the water. It must also be noticed that Kangshan basin is used as a flood retention basin and it had not been flooded since 1998.

C. The Poyang Hu major basin can be divided in two sub-systems

(i) Gan and Fuhe delta and Poyang Hu, the south-western part of Poyang Hu

Gan and Fuhe delta can be divided into 3 parts drained by 3 different branches of the Gan Jiang. The Northern branch of the Gan Jiang, with Lao Jiang, flow directly into the channel linking Poyang Hu to Changjiang. In this sector of the delta, the lakeshore shows a strong hydrological dynamic. It seems that flows fill the lakeshore basin only when the channel is full.

In the central part of the delta, the lakeshore presents a less pronounced dynamic than in its northern and southern parts. Flows of the central branch of the Gan Jiang fill directly the principal tank of the Poyang Hu.

The southern part of the delta, drained by the third branch of the Gan Jiang, the Xin Jiang and the Fuhe Jiang, presents the strongest dynamic of the lakeshore. Water flows coming from these rivers appear to be concentrated into a transfer channel which bypasses to the north the major Poyang Hu tank before flowing directly into the channel linking Poyang Hu to Changjiang. This lakeshore part might fill when the transfer channel is blocked by the infilling of the Poyang Hu.

(ii) Xi He and Dalianzi Hu, the north-eastern part of the Poyang Hu

This area is drained by Po Jiang and Xi Jiang. The water tank of Xi He, the major perennial water body of this area, collects flows from the two main rivers. Its lakeshores show the strongest dynamics in the north-western part of the Xi He and also in lateral valley ends.

The Dalianzi Hu is a lateral lakeshore of the Po Jiang which is not directly supplied by this river but indirectly by overflow of the Xi He and Poyang Hu. The Dalianzi Hu presents the strongest yearly submersion dynamics in this Poyang Hu part.

This spatial recognition of Poyang Hu sub-systems based on yearly submersion time estimation is the first step for the development of hydrodynamic models. Over such areas where hydrophile flora and fauna species depend on the presence of water, the proposed hydrological sub-systems defined by the submersion time map are key elements in a sensitive ecosystem dynamic characterization. For example, the proposed C.1 area corresponding to Gan and Fuhe delta provides habitats for rare migratory birds living through winter and it is one of the major national nature reserves declared as a Ramsar site. This type of ecosystem is very sensitive to wetland dynamic disturbances such as the changes in the spatial distribution of flooded areas and the time of submersion within a year.

The spatial distribution of water dynamics, given by the submersion time map, also provides essential information as part of wetland restoration policy monitoring and management, through for example the identification of hydrologically and ecologically sensitive areas.

V. CONCLUSION

For the first time, a large inland water body was monitored using a large amount ENVISAT low and medium resolution data, both radar and optical, during two and half years (from January 2004 to June 2006). These 64 datasets were combined and integrated based on an original approach in order to monitor Poyang Hu area variations between January 2004 and June 2006; to estimate the yearly submersion time of the lake, and to spatially differentiate Poyang Hu sub-systems.

Poyang Hu area variation monitoring, initiated by Qian in 2003 (Qian, 2006) using MODIS data, is now enriched with a time series to June 2006 with ENVISAT data. Our analysis shows that the infilling occurred over 4 months, generally between

March and June. Lake extent grew regularly to reach its annual maximum during July and August. The draw-off of the lake was faster (2 months) and occurred between September and the beginning of November. The entire Poyang Hu flooded area derived from the estimation of submersion time reaches 3436.2 km^2 which is 332.4 km^2 more than the largest instantaneous observed flood between January 2004 and June 2006, hence leading to the conclusion that the flood water bodies move within the basin depression system over time. These results highlight the great potential of ENVISAT, and Medium Resolution Earth Observation data, in general for monitoring large inland water bodies.

Poyang Hu was divided into 3 major hydrological sub-systems: the channel linking Poyang Hu to Changjiang, the small lateral lakes, and the major basin which was itself divided into 2 sectors according to a SE-NW axis (Gan delta and Poyang Hu in the south-west and Xi He and Dalianzi Hu in the North-East). Defined from the estimates of submersion time, these hydrological sub-systems are closely related with particular ecosystem characteristics and constitute a preliminary step in understanding the lake's hydrodynamic model.

Further steps would be the integration of extreme hydrological years characterizing drought periods and major floods. Accordingly, ERS and SPOT 4 data acquired during 1998's dramatic flooding are being processed. Also, the 2006 flood season around Poyang Hu was marked by very low water levels, reaching levels normally seen at the end of the draw-off period. This period was covered by ENVISAT ASAR and MERIS, and the integration of these two opposite lake states would allow an improved characterization of Poyang Hu water variation patterns.

The approach applied to detect the Poyang Hu can be transferred worldwide in a global climate change context over numerous large sensitive areas. The other similar large flood-prone basins in Asia with similar characteristics such as Dongting Hu in China, as well as Tonle Sap in Cambodia, Cagayan basin in Philippines, could be monitored too. Vast watersheds in Austral and Oriental Africa could be also considered following the same approach. In addition, this method can be adapted to monitor large river dynamic and floods such as the Lena River or the Ganges' and the Brahmaputras' lower basins.

These goals are attainable. The required Earth Observation databases and derived products (such as DEM's) are now available. The amount of data available is already sufficient for initiating such monitoring worldwide on considering only the European sensor data archives (ERS, ENVISAT ASAR and optical medium resolution). Planned for 2010's, ESA's Sentinel 1 and 2, comprising a large field optical sensor and a SAR sensor, will allow a daily revisit over the same area. Thus, the offer of high and medium resolution data will be really improved and the monitoring of large flood prone water basins would reach an operational stage.

ACKNOWLEDGMENTS

This work was realized within the framework of the Sino-European joint research (ESA-NRSCC) DRAGON project 2551 and supported by ESA's *"Support Training of Young European Scientists"* through a grant allocated for the project *"Assessment of the synergistic exploitation of ENVISAT ASAR and MERIS data for Rapid Plain Flood Mapping"*.

Authors are grateful for the ESA staff, more particularly for Rita Malosti who very kindly and very professionally/ efficiently provides lot of advice and help for data ordering. Thanks are also due to Henri LAUR, the ENVISAT mission manager, and the EO Helpdesk for their quick and considerable help. Authors would also like to thank Dr Christine KING (BRGM) for her support through the Sino-French WARM cooperation programme.

Landsat mosaics have been obtained, thank to the GLM facilities of the Maryland University, USA. Authors would finally associated SERTIT colleagues for all fruitful and animated discussions.

REFERENCES

[1] Desnos Y L., Bergquist K., Li Z., 2004, The Dragon programme: ESA and China cooperate in earth observation. E.S.A bulletin (E.S.A. bull.) ISSN 0376-4265 European Space Agency bulletin 2004, n°119: 22–28.

[2] Desnos Y L., Li Z., 2006, EO Science and Applications Development in P.R. China. Proc. 2005 Dragon Symposium "Mid-Term Results", Santorini, Greece 27 June–1 July 2005, ESA SP-611: IX–XXV.

[3] Yésou H., Li J., Li J., Wang X., Yida F., Wang Y., Huang S., Xin J., de Fraipont P., 2004, Assessment of the Synergistic Exploitation of ENVISAT ASAR and MERIS Data for Plain Flood Rapid Mapping: a Part of the Dragon Flood Project. ENVISAT Symposium Salzburg 6–10 September 2004.

[4] Li J., Yésou H., Huang S., Li J., Li X., Xin J., Wang X., Andreoli R., 2006, ENVISAT ASAR medium and high resolution images for Near Real Time flood monitoring in China during the 2005 flood season. Proc. 2005 Dragon Symposium "Mid-Term Results", Santorini, Greece 27 June–1 July 2005, ESA SP-611: 213–226.

[5] King C., Li J., Costes M., Yésou H., Prinet V., 2004, WARM Water Risk. Management Research Network CEOS meeting Information, Products and Services for Disaster Management, Beijing China, 17–19 November 2004.

[6] Yésou H., Li J., Wang Y., Xin J., Clandillon S., de FRAIPONT, P., 2004, Assessment of CHRIS PROBA data for land cover derivation and flood mapping. Application over the Dongting-Poyang lake sectors and to the Songhuajiang River(China). Proceedings of the 2nd ESA Chris/Proba workshop, Frascati, Italy, 28–30 April 2004.

[7] Andreoli R., Yésou H., 2006, Monitoring water level seasonal variations of large natural lake exploiting ENVISAT ASAR low resolution time series: application to Poyang Lake (P.R. China)

during the 2004–2005 hydrological period. Proc. 2005 Dragon Symposium "Mid-Term Results", Santorini, Greece 27 June–1 July 2005, ESA SP-611: 213–226.

[8] Pedersen L T., Saldo R., 2005, Experience with the near real time distribution of Envisat ASAR data to end-users. Proc. of the 2004 Envisat & ERS Symposium, Salzburg, Austria 6–10 September 2004, ESA SP-572.

[9] Jiangxi Meteorological Bureau: http://www.weather.org.cn

[10] Shankman D., Liang Q., 2003, Landscape Changes and Increasing Flood Frequency in China's Poyang Lake Region. The Professional Geographer, 55(4): 434–445.

[11] Shankman D., Keim B D., Song J., 2006, Flood Frequency in China's Poyang Lake Region: Trends and Teleconnections. Int. J. Climatol. 26: 1255–1266.

[12] Jiang L., Yu X., Zhao H., Zhou Y., 2005., China's Wetlands Restoration around Poyang Lake, Middle Yangtze: Evidences from Landsat TM/ETM Images. Proc. of Geoscience and Remote Sensing Symposium, IGARSS '05, IEEE International Volume 4, 25–29: 2387–2389.

[13] Smith L C., 1997, Satellite remote sensing of river inundation area, stage, and discharge: a review. Hydrological Processes, Vol. 11 (10): 1427–1439.

[14] Tholey N., Clandillon S., de Fraipont P., 1997, The contribution of spaceborne SAR and optical data in monitoring flood events: examples in Northern and Southern France. Hydrological Processes, 11: 1409–1413.

[15] Laugier O., Fellah K., Tholey N., Meyer C., de Fraipont P., 1997, High Temporal Detection and Monitoring of Flood Zone Dynamic using ERS Data around Catastrophic Natural Events: the 1993 and 1994 Camargue Flood Events. Proc. of the third ERS Symposium, ESA SP-414(1): 559–564.

[16] Chen D., Huang S., Yang C., 1999, Construction of watershed flood disaster management information system and its application in great flooding of Yangzi River in 1998. Journal of Chinese Geography.

[17] Mahmood A., Parashar S., Giguère C., 1999, Radarsat 1 background mission data for flood monitoring. Proc. IGARSS, Hamburg, Germany.

[18] Sarti F., Inglada J., Landry R., Pultz T., 2001, Risk management using Remote Sensing data moving from scientific to operational applications. Proc. of X SBSR April 23–27, 2001, Brasil.

[19] Yésou H., Chastanet P., de Fraipont P., Dossmann P., Stock N., Béquignon J., 2001, Mapping Floods in France. Backscatter, 12 3: 23–26.

[20] Xu M., Li J., Huang S., 2003, Quickly Monitoring and Evaluation of Floodwater and Waterlogging Disaster in Huaihe River Remote Sensing and GIS Technology. Water Resource and Hydropower Engineering, 34: 7.

[21] Zhou C., Luo J., 2000, Flood monitoring using multi-temporal AVHRR and RADARSAT imagery. Photogrammetric Engineering and Remote Sensing, 66 (5): 633–638.

[22] Li J., Huang S., 2003, Guide for Application of "3S". in Water Resources, China WaterPower Press.

[23] Islam M., Sado K., 2000, Flood hazard assessment in Bangladesh using NOAA AVHRR data with geographical information system. Hydrological Processes, Vol. 14(3): 605–620.

[24] Liu Z., Huang F., Li L., Wan E., 1999, Dynamic monitoring and damage evaluation of flood in north-west Jilin with remote sensing. GIS development. ACRS 1999.

[25] Liu Z., Huang F., Li L., Wan E., 2002, Dynamic monitoring and damage evaluation of flood in north-west Jilin with remote sensing. International Journal of Remote Sensing, Vol. 23(18): 3669–3679.

[26] Gao Y., Yu J., Li L., Wang C., Zheng Y., 2001, NOAA AVHRR data for Yangtze flood monitoring in 1998. Proc. Geoscience and Remote Sensing Symposium, IGARSS '01. 2001 IEEE International, I: 138–140.

[27] Tan Q., Bi S., Hu J., Liu Z., 2004, Measuring Water Level Using Multi-source Remote Sensing Images Combined with Hydrological Statistical Data. Proc. Geoscience and Remote Sensing Symposium, IGARSS '04. 2004 IEEE International, VII: 4885–4888.

[28] Yésou H., Chastanet P., Fellah K., Jeanblanc Y., de Fraipont P., Béquignon J., 2000, Contribution of ERS SAR images and ERS coherence data to a flood information system on the Meuse basin–France. Proc. of ERS-ENVISAT Symposium "Looking at our Earth for the New Millennium" (16–20/Ocr. 2000 Gothenburg) SP-461: 9p.

[29] Seiler R., Csaplovics E., 2003, Monitoring landcover changes of the Niger inland delta(Mali) by means of ENVISAT-MERIS data. ESA-ESRIN MERIS user workshop, 10–13 November 2003: 10 p.

[30] Qian L., 2006, Monitoring Area Variation and Sedimentation Patterns in Poyang Lake, China Using MODIS Medium-Resolution Bands. International Institute for Geo-information Science and Earth Oberservation thesis, Netherlands: 72 p.

[31] ESA, 2002. ASAR product Handbook: 543 p.

[32] ESA, 2004. MERIS product Handbook, Issue 1.2: 517 p.

[33] ESA, 2005. BEST Basic Envisat SAR Toolbox User Manual. Version 4.0.2.: 190 p.

[34] ESA, BEAM Handbook: www.brockmann-consult.de/beam/documentation.html

[35] Smith L C., 1997, Satellite remote sensing of river inundation area, stage, and discharge: a review. Hydrological Processes, Vol. 11 (10): 1427–1439.

[36] Andreoli R., Li J., Yésou H., 2006, ASAR and MERIS ENVISAT Low and Medium Resolution Product Time Series Exploitation for Large Flood Plain Monitoring(Poyang Lake, P.R. China) Within the Flood DRAGON Project. Proc. 2006 Dragon Symposium, Lijiang, China 10 July–14 July 2006.